Reliability Engineering and System Safety 267 (2026) 111855

Contents lists available at ScienceDirect

Reliability Engineering and System Safety

journal homepage: www.elsevier.com/locate/ress

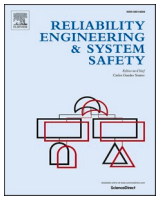

Resilience improvement framework based on strategy optimization of power systems to typhoons

Xiao Liu [a,b,c], John S. Owen [b], Qiang Xie [a,*], Tiantian Wang [a,b,c]

[a] College of Civil Engineering, Tongji University, Shanghai 200092, China
[b] Faculty of Engineering, University of Nottingham, Nottingham NG7 2RD, UK
[c] State Grid Electric Power Engineering Research Institute Co., Ltd., Beijing 102401, China

ARTICLE INFO

Keywords:
Functional time-varying curve
Improvement strategies
Optimization algorithm
Power system
Resilience assessment under typhoons

ABSTRACT

Typhoons severely damage power systems and cause them to recover slowly. To improve the power systems resilience to typhoons, this paper first evaluates the operational states of components within power systems based on a typhoon wind-field model and infrastructure fragility curves. The network functional model was built using undirected weighted graphs and adjacency matrices. A quantitative resilience assessment of power systems was achieved through functional time-varying analysis. Subsequently, a resilience improvement framework based on strategy optimization in power systems was proposed. The framework includes two optimization algorithms and four strategies. A wind-resistant improvement strategy optimization algorithm was proposed based on economic constraints. A functional recovery strategy optimization algorithm was proposed under resource constraints. The recovery efficiency was increased by assessing the repair priority of infrastructure and resource utilization. The effectiveness and interrelationships of these strategies are evaluated based on resilience metrics. Taking a typical power-network reliability test system as a case study for resilience improvement strategies under typhoon disasters. The optimal combination of multi-dimensional strategies was determined based on economic budgets and resource constraints, thereby achieving maximum resilience improvement for power systems under various engineering scenarios and typhoon events.

1. Introduction

Power systems are critical lifeline networks in urban areas. A damaged power system can severely disrupt the normal operation of other networks such as transportation, water supply, and communications. However, the operation of power systems has been severely damaged during past typhoon disasters [1,2]. This highlights the fragility of power systems under the influence of typhoons. Therefore, assessing the power system's resistance to typhoons and identifying effective measures for recovery are key research issues to ensure the safety of power systems.

Resilience refers to a system's ability to withstand and recover from external disturbances. Owing to its applicability to disaster resistance assessments in engineering networks, the concept of resilience has been widely used in urban systems such as water supply, transportation, and healthcare [3–5]. Previous studies have summarized both qualitative and quantitative assessment methods for resilience and have developed resilience assessment frameworks suitable for urban engineering networks [6–9]. In power systems, many researchers have conducted studies on the disaster resilience of power infrastructure, including the fragility of transmission tower systems and the functional state assessment of substations [10–13]. These studies have laid a foundation for resilience assessment in regional power grids [14]. Based on the motion characteristics of typhoon disasters, scholars have developed typhoon path simulation models [15] and evaluated the impacts of typhoons on power systems [16–18]. Additionally, implementing early warning systems for power systems through meteorological monitoring is also a crucial stage in resilience assessment [19]. To achieve the wind resilience assessment for power systems, Ouyang et al [20] developed a probabilistic method to assess the hurricane resilience of power systems. However, their fragility analysis primarily relies on the HAZUS database, and they have not yet established a method for determining the operational states of multi-operational-state infrastructure. Espinoza et al [21] conducted disaster simulations for power systems based on disaster characteristics, but they overlooked the variability in the intensity and direction of disasters at different infrastructure locations. Liu

* Corresponding author.
E-mail address: qxie@tongji.edu.cn (Q. Xie).

https://doi.org/10.1016/j.ress.2025.111855
Received 19 October 2024; Received in revised form 11 September 2025; Accepted 26 October 2025
Available online 26 October 2025

et al [22] proposed system and component resilience assessment indices but neglected the possibility of multiple operational states for different types of infrastructure. Therefore, a preliminary resilience assessment framework for power systems has been established, but the issues of infrastructure operational states and the varying impact of typhoons on components remain unresolved. These challenges have also been present in resilience assessments for natural disasters such as earthquakes and ice storms [23]. Therefore, we focus on the operational states of power system infrastructure, emphasizing the impact of typhoon wind-field intensity and direction on infrastructure. The accuracy of the results is improved by refining the power system resilience assessment framework, thereby laying the foundation for the resilience enhancement strategies.

Many measures are used to enhance the resilience of power systems. Fang and Wu et al. took into account uncertainties during the design, operation, and recovery phases of the engineering system. This contributes to the research progress in improving the resilience of power systems [24,25]. Mahzarnia [26] summarized the resilience improvement techniques and measures for different stages of power systems, classifying resilience measures into two general categories: "preservation measures" and "recovery measures." Most resilience enhancement strategies can be considered from these two aspects. In terms of preservation measures, Tari and Hou et al [27,28] have considered the upgrading, retrofitting, and reinforcement of utility poles to improve the disaster resistance of the system. However, they did not discuss the identification of critical components and the effectiveness of reinforcing multiple components together. Zhou et al [29] explored the optimal distributed generator rescheduling strategy, and Yuan et al [30] considered hardening and distributed generation resource placement. But they overlooked the constraints of regional economic and resource conditions. The existing conditions may not meet the needs of actual engineering optimization. Although Yang et al [31] evaluated transmission line reinforcement measures considering economic costs, they adopted a method combining subjective scoring and objective optimization without conducting a comprehensive and detailed screening of the optimal solutions. In terms of recovery measures, Shi et al [32] summarized resilience-oriented post-disaster restoration scheduling and resource allocation. However, they did not study the scheduling of repair crews or methods for optimizing repair paths. Liang et al [33] built a three-stage optimal resilience enhancement dispatch framework to withstand extreme typhoon events, but they neglected the impact of coordination between various strategies and the constraints of resource conditions. In addition, some scholars have assessed the importance of infrastructure repair based on factors such as the load capacity of power infrastructure, the number of people served, or repair efficiency [28,34–36]. But they overlooked the interconnection between infrastructure and power systems. These factors result in the measures they have adopted not necessarily being the optimal recovery strategies [37]. Therefore, many issues remain to be addressed regarding resilience improvement measures in power systems under typhoons. Therefore, in this research context, we aim to find optimization methods for resilience improvement strategies that overcome the limitations posed by economic and resource constraints [31,38]. Furthermore, the interrelationship between various strategies is important. These issues are addressed in this study.

Several research gaps can be identified in the aforementioned resilience assessment for power systems:

1) Previous studies have considered the basic parts of resilience assessment frameworks, including typhoon models, component fragilities, and network models. However, the structural and operational characteristics of infrastructure are different [10,12], leading to distinct methods for evaluating the operational states of different types of infrastructure [20,22]. Additionally, both typhoon trajectories and the power system recovery process are dynamically changing; the method for quantifying the time-varying operational states of power systems remains unclear. This directly affects system resilience assessment results and the determination of improvement measures under disasters.
2) Resilience improvement measures for power systems focus on the reinforcement of infrastructure and the prioritization of post-disaster recovery paths. However, researchers overlook the interconnections between different infrastructures [27,28,34]. Additionally, there are mutual constraints between various resilience enhancement measures [31,33]. Therefore, it is crucial to identify the key infrastructure within power systems and clarify the coordination and synergy between different strategies.
3) Many scholars have proposed methods for evaluating resilience enhancement strategies; they focus on the impact of these strategies on system functional states and resilience. However, they have not yet considered the limitations imposed by resource conditions and economic demands [30,32,35]. These directly affect the accuracy and applicability of the strategies. Therefore, finding the optimal resilience improvement strategies under varying economic and resource constraints can be challenging.

Based on the identified knowledge gaps, the objectives of this study are to:

(1) evaluate the power system's operational states and resilience under typhoon conditions;
(2) propose multidimensional resilience improvement strategies based on engineering requirements;
(3) identify critical infrastructure for wind-resistant retrofitting and post-disaster recovery using strategy optimization algorithms;
(4) determine the optimal combinations of resilience improvement strategies under economic and resource constraints.

In this study, we propose a quantitative evaluation method for the operation of electrical infrastructure and use an adjacency matrix to construct a network functional model of power systems. The functional time-varying process of power systems is simulated based on typhoon trajectories. Subsequently, multidimensional resilience improvement strategies are proposed. The effectiveness and interrelationships of these strategies are evaluated based on resilience metrics. The operation of a typical power-network test system is analyzed to clarify the resilience improvement strategies under typhoon disasters. The applicability of the proposed framework and the importance of the strategies are verified. The main contributions are as follows:

1) We establish a quantitative resilience assessment method for power systems under typhoon conditions. The time-varying states of system functional loss and recovery are clarified.
2) We propose a resilience improvement assessment framework for power systems. Four dimensions of resilience enhancement strategies before and after typhoons are considered.
3) We develop resilience enhancement strategy optimization algorithms to evaluate the effectiveness of resilience improvement of power systems under specific typhoon scenarios.
4) We identify the inter-coordination relationships between resilience improvement strategies. The optimal combinations of resilience improvement strategies are determined.

2. Resilience assessment of power systems to typhoon winds

The resilience assessment method for power systems under typhoons consists of four parts, as shown in Fig. 1. First, the characteristic parameters of the typhoon's movement process are clarified, including the typhoon's moving track and speed, as well as the variations in the central pressure and latitude. Next, a network functional model of power systems is constructed. The operational states of various infrastructure under typhoons are evaluated by building an undirected weighted graph

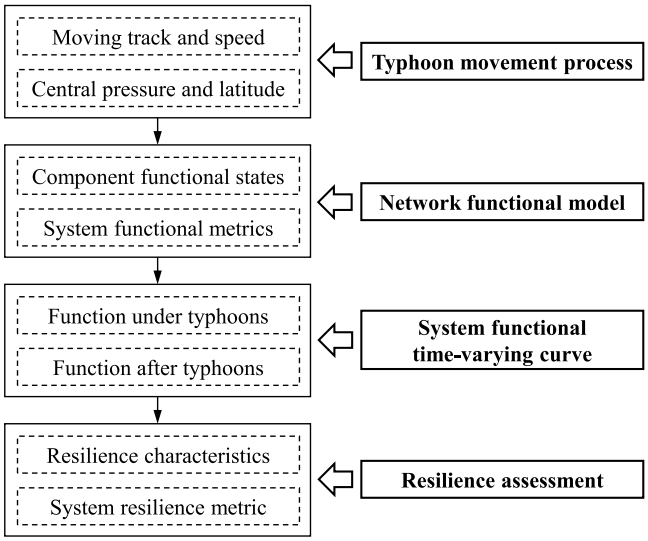

Fig. 1. Resilience assessment framework for power systems under typhoons.

and storing infrastructure's functionality and connectivity information in an adjacency matrix. System functional metrics are set to quantitatively assess the operation of power systems. Subsequently, the functional loss under typhoons and post-disaster functional recovery of power systems are evaluated to establish the system's functional time-varying curve. Finally, the functional time-varying curve is combined with resilience characteristics. Resilience metrics are proposed to quantitatively assess the resilience of power systems.

2.1. Typhoon movement process

A typhoon wind-field model is constructed to assess the impact of typhoons on power infrastructure. We need to calculate the wind speed $V_{h,r}$ at a height h when the distance from the typhoon center is r. The gradient wind speed is calculated based on the boundary layer model to obtain $V_{h,r}$, as shown in Eq. (1) [39]. Here, $V_{\max}$ represents the maximum wind speed of the typhoon, $r_{\max}$ is the distance from the typhoon center to the region of strongest winds, h_g is the gradient height, and α is the roughness index, with a value of 0.09 for the sea and 0.18 for the land.

$$V_{h,r} = \begin{cases} V_{\max} \times \dfrac{r}{r_{\max}} \times \left(\dfrac{h}{h_g}\right)^{\alpha} & r \le r_{\max} \\ V_{\max} \times \left(\dfrac{r_{\max}}{r}\right)^{0.7} \times \left(\dfrac{h}{h_g}\right)^{\alpha} & r > r_{\max} \end{cases} \tag{1}$$

Referring to the Batts wind-field model for assessing wind speeds in various regions of the wind field [40,41], $r_{\max}$ is calculated, as shown in Eq. (2).

$$r_{\max} = \exp\left(-0.1239\left(\sqrt{H_{out} - H_{center}}\right)^{0.6003} + 5.1034\right) \tag{2}$$

Here, H_{out} represents the atmospheric pressure in the typhoon's outer region, typically taken as 1013 hPa, and H_{center} denotes the atmospheric pressure at the typhoon center. The $V_{\max}$ is obtained through Eq. (3). In this equation, k is a constant coefficient, generally taken as 6.72, ω is the Earth's rotational angular velocity, typically 7.292×10^{-5}rad/s, ψ represents the geographical latitude, and V_m is the typhoon's movement speed.

$$V_{\max} = 0.865\left(k\sqrt{H_{out} - H_{center}} - r_{\max}\omega\sin\psi\right) + 0.5V_m \tag{3}$$

2.2. Network functional model

2.2.1. Component functional states

Fragility curves were employed to measure the operational reliability of the infrastructure's operation at different intensity measures (IM). Because wind speed and direction are primary factors affecting the performance of infrastructure, they are used as the parameters for measuring typhoon intensity. A limit state criterion (*LSC*) is established to determine the operational state of the infrastructure. When the functional state (*FS*) of the infrastructure exceeds the *LSC*, the infrastructure can be considered to have failed; otherwise, it is working. P_f is used to measure the probability that the *FS* exceeds the *LSC* when the IM equals x, this indicates the failure probability of the infrastructure. The previous literature indicates that the fragility curves of infrastructure follow a log-normal distribution cumulative function, characterized by a median μ and a log standard deviation β, as shown in Eq. (4). Here, Φ () represents the standard normal cumulative distribution function.

$$P_f(FS > LSC|\mathrm{IM} = x) = \Phi\left(\frac{\ln(x/\mu)}{\beta}\right) \tag{4}$$

In power systems, power plants and substations are complex electrical transmission networks characterized by multiple operational states. The operational states include the proportion of equipment damage, the ratio of power load, or the number of output terminals operating normally. Therefore, these types of infrastructure have various limit state criteria for assessment. To assess the performance of infrastructure with multiple-level operational states, it is assumed that the infrastructure has S levels of working states (from F_1 to F_S) with S corresponding criteria (from LSC_1 to LSC_S), These criteria can be used to determine whether the infrastructure is operational. The failure probability of the infrastructure can be derived using these criteria. The F_i inside the parentheses represents the operational state corresponding to the criteria LSC_i. Where F_1 represents complete failure with a value of 0, F_i denotes the operational state at level i, F_S denotes good operating conditions with a value of 1, and LSC_i represents the i-th criterion. If the infrastructure's performance $FS \ge LSC_i$, the infrastructure can be considered to be working; if $FS < LSC_i$, the infrastructure can be considered to have failed.

If we assume the IM to be equal to x, then $P_{f,1}$ represents the failure probability when LSC_1 is the criterion, i.e., the probability of complete failure; $P_{f,i}$ denotes the failure probability when LSC_i is the criterion, i.e., the probability that working state $FS < LSC_i$; $P_{f,S}$ represents the failure probability when LSC_S is the criterion, i.e., the probability that the infrastructure is not fully operational. Consequently, $(P_{f,\,i+1} - P_{f,\,i})$ denotes the probability that the infrastructure is in an operational state F_i, and $(1 - P_{f,\,S})$ represents the probability that the system is fully operational. The probability-weighted average of the working state can be calculated based on the infrastructure performance and corresponding probabilities. Finally, the operational state of the infrastructure when IM $= x$ is represented as k (IM $= x$) in Eq. (5).

$$k(IM = x) = \sum_{i=1}^{S-1}\left(P_{f,i+1} - P_{f,i}\right)F_i + \left(1 - P_{f,S}\right)F_S \tag{5}$$

Furthermore, the structural state of transmission towers can be established using criteria based on plastic behavior or buckling. However, the operational state of the transmission line can only be determined by its ability to transmit power. Therefore, when the functional state (*FS*) of a transmission tower exceeds the *LSC*, it is considered that the operation of the transmission tower is lost.

2.2.2. System functional metrics

The power system is a complex undirected power transmission network, where "undirected" means that power can flow bidirectionally. Specifically, the transmission direction of power in a transmission line within the power system mainly depends on power flow and network

connectivity status. It is also affected by the system's power generation and load distribution. Therefore, power transmission is characterized by dynamics and reversibility. Therefore, an undirected weighted graph $G(V, E)$ is used to represent the power system's operation. This can reflect the properties of an "undirected graph" in graph theory. Here, V denotes a finite set of vertices, it includes power plants, substations, and bus nodes, and E represents the set of edges connecting the vertices, which corresponds to all transmission lines. Subsequently, an adjacency matrix **A** is employed to consolidate and collect the characteristic parameter information from the undirected weighted graph, thereby facilitating the simulation of power systems under typhoons. The elements a_{ij} of the adjacency matrix **A** indicate the adjacency relationship between vertices V_i and V_j in $G(V, E)$. If there is no connection between vertices V_i and V_j, then $a_{ij} = 0$. If there is a connection between vertices V_i and V_j, a weight γ_{ij} is assigned to the edge connecting these vertices, where γ_{ij} represents the length of the edge between vertices V_i and V_j, as shown in Eq. (6).

$$a_{ij} = \begin{cases} \gamma_{ij}, & if\left(V_i, V_j\right) \in E \, or < V_i, V_j > \in E \\ 0, & if\left(V_i, V_j\right) \notin E \, or < V_i, V_j > \notin E \end{cases} \tag{6}$$

Based on the undirected weighted graph for power systems, three functional parameters were proposed for quantitative evaluation of the system's operational state: power transmission efficiency, power transmission reliability, and power load capacity. Power transmission efficiency (K_{TE}) refers to the speed and amount of energy loss during power transmission within power systems. Power transmission reliability (K_{TR}) represents the reliability of power transmission from power plants to load hubs. Power load capacity (K_{LC}) refers to the maximum amount of transmitted power load, as shown in Eq. (7).

$$\begin{cases} K_{TE} = \dfrac{1}{N(N-1)} \displaystyle\sum_{i \neq j} \dfrac{1}{D_{ij}} \\ K_{TR} = \dfrac{1}{N_L} \displaystyle\sum_{i \in V} \dfrac{N_p^i}{N_p} \\ K_{LC} = \displaystyle\sum_{i \in V} L_i k_i + \sum_{j \in V} L_j k_j + \sum_{u \in V} L_u \end{cases} \tag{7}$$

Here, N represents the total number of nodes in the finite set $G(V, E)$; D_{ij} denotes the shortest distance between nodes V_i and V_j in the network; N_L denotes the number of load nodes in power systems, which include substations and bus nodes. N_p denotes the number of power plants in power systems; N_p^i represents the number of power stations connected to the load node i; L_i, L_j, and L_s represent the active power outputs of the i-th power plant, the j-th substation, and the s-th bus node, respectively. k_i and k_j represent the functional state (FS) of the i-th power plant, and the j-th substation, respectively.

To comprehensively consider the impact of the three-dimensional parameters on the operational state of power systems, each set of functional parameters is assigned a weight coefficient λ. By comparing the changes in the functional parameters of power systems before and after a typhoon, a quantitative assessment of the functionality after the disaster is achieved, as shown in Eq. (8). Here, $K_{i,b}$ and $K_{i,a}$ represent the functional parameters before and after a typhoon, respectively.

$$K = \lambda_1 \frac{K_{TE,a}}{K_{TE,b}} + \lambda_2 \frac{K_{TR,a}}{K_{TR,b}} + \lambda_3 \frac{K_{LC,a}}{K_{LC,b}} \tag{8}$$

2.3. System functional time-varying curve

Functional states of power systems exhibit two stages: functional loss and functional recovery. To quantitatively assess the time-varying process of power systems, two time-varying parameters from both function and time are proposed. In the functional loss stage, the time-varying analysis focuses on the impact of typhoon intensity and movement path on the power infrastructure. Because the functionality of power systems continuously declines under a typhoon, we assume a linear decrease in functionality between any two monitoring intervals. In the functional recovery stage, the time-varying analysis emphasizes the impact of repair resource conditions and strategies on power systems. When the functionality of infrastructure is restored, the infrastructure can immediately reconnect to the network, thereby partially restoring the functionality of a power system. As a result, the functionality recovery of the power system exhibits a stepped-ascending process.

The functional time-varying analysis of power systems is divided into four parts, as shown in Fig. 2. In the functional loss stage, real-time monitoring of the typhoon provides the movement characteristic parameters of the typhoon. Based on the fragility parameters of the infrastructure, iterative simulations are conducted under the typhoon to output the system residual function and the monitoring time parameters. Subsequently, the network functional model is updated based on the performance of the infrastructure, and further typhoon simulations are carried out. Finally, the time-varying curve of the functional loss process of the power system, $K_{res}(t)$, is determined based on the time-varying parameters.

In the functional recovery stage, a functional recovery path is established based on the damaged infrastructure. Repairs are conducted according to the repair steps. Then, the functional recovery simulations are conducted to output the system recovery function and the repair time parameters. The functional model of the repaired power system is updated, and further functional recovery simulations are performed. Finally, the time-varying curve of the functional recovery process of the power system, $K_{rec}(t)$, is determined.

2.4. Resilience assessment

The functional time-varying curve of power systems aligns with the concepts and characteristics of resilience. The functional loss stage of power systems reflects its ability to resist typhoons, this process is represented as wind robustness in resilience assessment. The functional recovery stage reflects its post-disaster recovery capability; this process is represented as recovery rapidity in resilience assessment. Currently, resilience assessment approaches for engineering networks are diverse and multifaceted, such as the center of resilience, the resilience bandwidth, and the standardized shadow area [42,43]. In this study, we mainly refer to Bruneau's concept of resilience, focusing on evaluating the resistance and functional integrity of engineering networks under disaster conditions. Therefore, based on the functional time-varying curve of power systems, resilience metrics are proposed, as shown in Eq. (9). Although this method has certain limitations, it still facilitates comparative analysis of multi-dimensional strategy optimization outcomes, and helps identify optimal strategies and measures under economic budget scenarios.

$$R = \int_{T_0}^{T_t} (100 - K_{res}(t))dt + \int_{T_t}^{T_r} (100 - K_{res}(T_t))dt + \int_{T_r}^{T_c} (100 - K_{rec}(t))dt \tag{9}$$

Where T_0 represents the time when the typhoon begins to affect power systems; T_t represents the time when the typhoon stops impacting power systems; T_r represents the time to start repair; and T_c represents the time to end repair. The duration of the typhoon's impact on power systems is given by T_t -T_0; the time for decision-making and deployment is given by T_r -T_t; and the recovery time of power systems is given by T_c -T_r. A larger resilience metric indicates weaker wind resistance and recovery of the power system, and a smaller resilience metric indicates stronger wind resistance capabilities of the power system.

3. Resilience improvement framework based on strategies optimization

Resilience improvement of power systems is primarily studied from two aspects: functionality loss and recovery time. Based on the stages

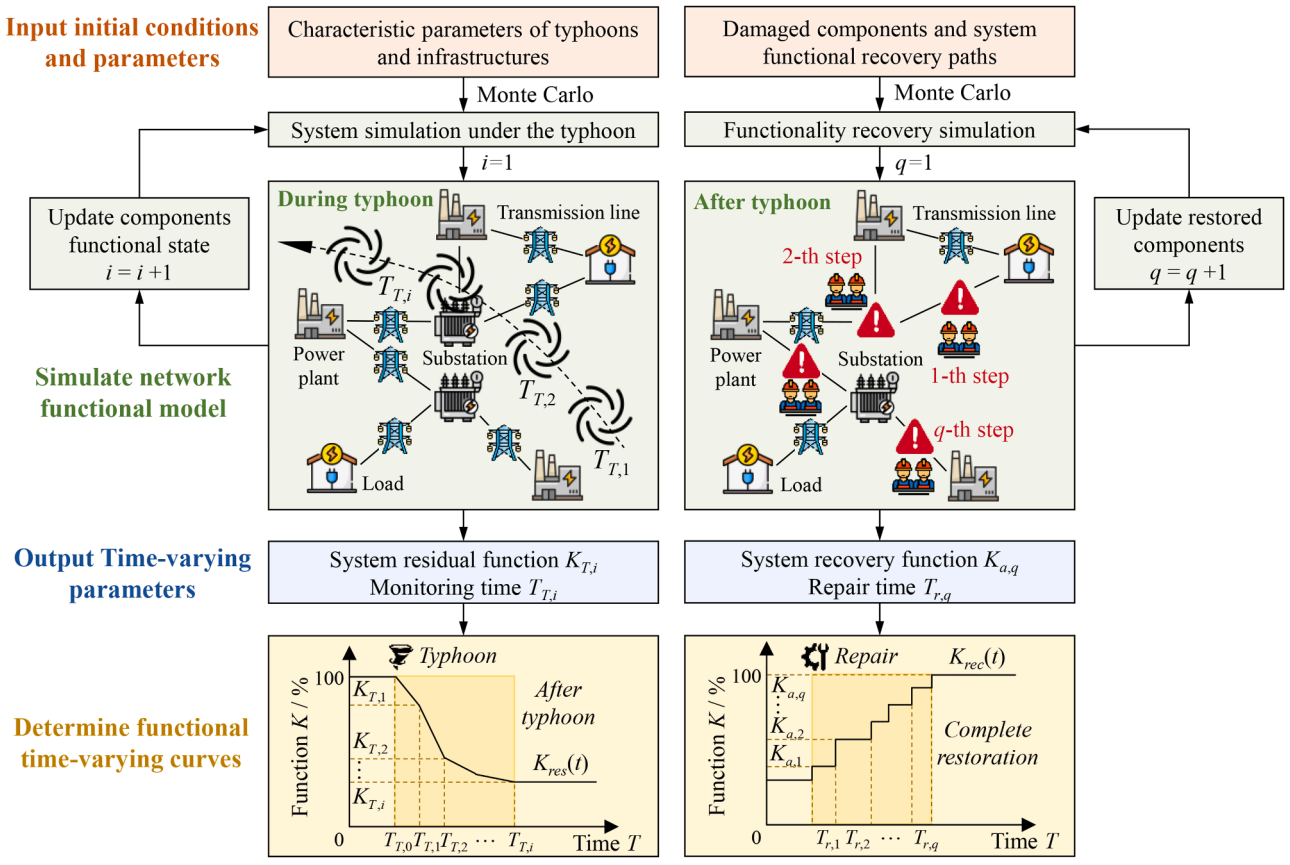

Fig. 2. Functional time-varying analysis diagram of power systems.

before and after the typhoon, four-dimensional strategies are proposed, as shown in Fig. 3.

The research focuses on optimizing resilience improvement based on the resilience characteristics of the four dimensions. In the pre-typhoon phase, the network's functional states and connectivity can be clarified. Spare lines are proposed to improve redundancy in the power transmission network. Additionally, identifying infrastructure fragilities and conducting wind-resistant reinforcement measures are crucial for

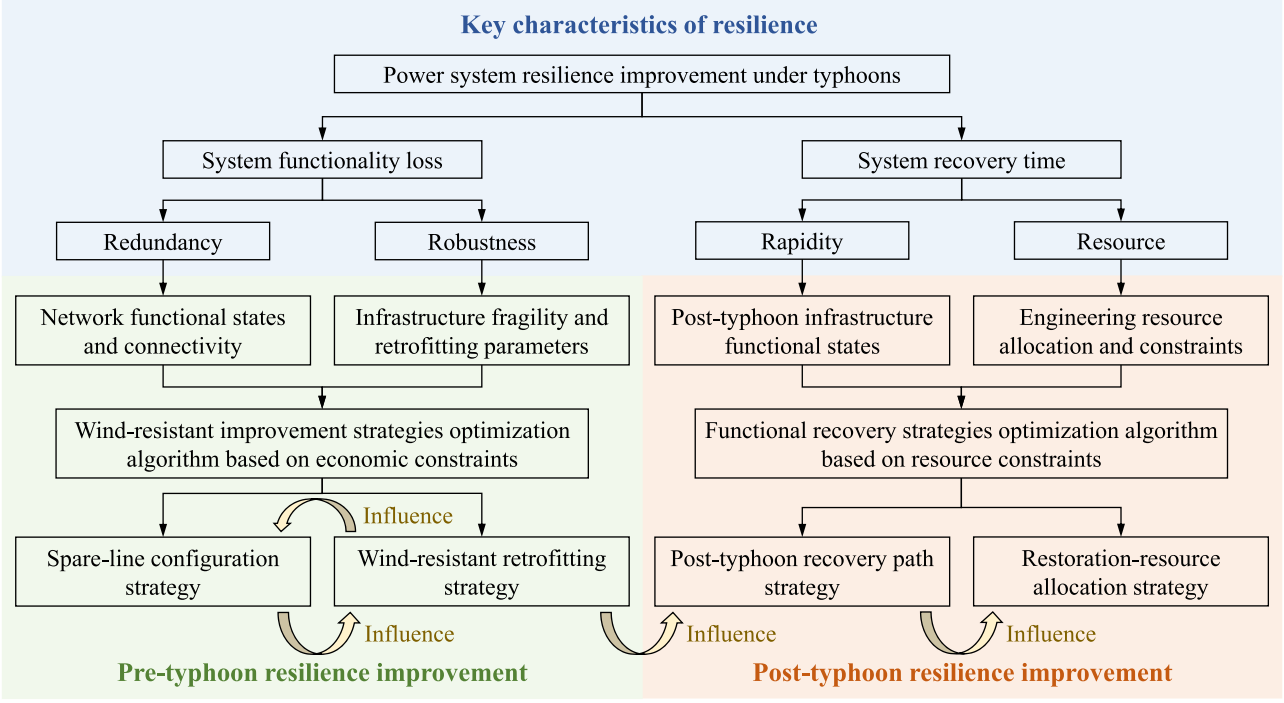

Fig. 3. Resilience improvement framework based on strategies optimization of power systems.

improving the system's robustness. An optimization algorithm for wind-resistant improvement strategies based on economic constraints is proposed. We aim at developing spare-line configuration strategies and wind-resistant retrofitting strategies. In the post-typhoon recovery phase, the damaged infrastructure and the constraints of engineering resources can be assessed. An optimization algorithm for functional recovery strategies based on resource constraints is introduced. The optimal post-typhoon recovery path and restoration-resource allocation strategies are determined, thereby enhancing the recovery efficiency of power systems.

In addition, various strategies have interrelation. The spare-line configuration strategies and wind-resistant reinforcement for infrastructure mutually influence each other, and the wind-resistant improvement strategies impact the post-typhoon operational states of the infrastructure. This will also influence the development of recovery paths and the allocation of restoration resources. Therefore, the coordination of these strategies is essential to achieving the maximum improvement of the power system's resilience.

3.1. Pre-typhoon resilience improvement

Spare-line configurations can increase redundancy in power transmission for certain areas. When power transmission is interrupted in specific regions, spare lines can take over part of the power transmission. However, the addition of spare lines requires economic and resource support, and excessive spare lines would significantly increase the budget and may not have a guaranteed impact on the system's performance. Therefore, it is crucial to identify weak points in the power transmission network and strategically place spare lines to maximize the system's wind resistance capacity.

Adding spare power transmission lines cannot improve the wind resistance of the infrastructure. Therefore, wind-resistant reinforcement should be applied to various types of infrastructure to reduce the risk of operational failure during typhoons. However, wind-resistant reinforcement consumes significant manpower, materials, and economic resources, it is impractical to reinforce all transmission lines and other infrastructure. Therefore, it is important to identify the most fragile infrastructure within the power system and carry out targeted reinforcements, thereby improving the operational reliability of the infrastructure.

Wind-resistance enhancement strategies can improve the power system's resilience; however, these strategies need to be optimized to enhance their effectiveness owing to economic constraints. Therefore, the resistance-based resilience metrics R_{res} are proposed to measure the wind resistance capacity of the power system under different strategies, expressed as follows:

$$R_{res} = \int_{T_0}^{T_t} (100 - K_{res}(t))dt \tag{10}$$

To optimize the wind-resistance enhancement strategies, we proposed a strategy optimization algorithm based on the particle swarm. In this algorithm, the improvement strategies are defined as particles. The specific implementation plans are represented by the particles' positions. The number of infrastructure components determines the dimensionality of the space in which the particles reside. By updating and iterating the positions and velocities of the optimal particles within the swarm, the optimization process is conducted to find the global optimum, resulting in optimized wind-resistance enhancement strategies. The iterations for particle positions and velocities are as follows.

$$\begin{aligned} X_i &= (x_{i1}, x_{i2}, \cdots, x_{id}, \cdots, x_{iD}), i = 1, 2, \cdots, N \\ V_i &= (v_{i1}, v_{i2}, \cdots, v_{id}, \cdots, v_{iD}), i = 1, 2, \cdots, N \end{aligned} \tag{11}$$

$$v_{id}^k = w v_{id}^k + c_1 r_1{}^k [pbest_i^k - x_{id}^k] + c_2 r_2^k [gbest^k - x_{id}^k] \tag{12}$$

$$x_{id}^{k+1} = x_{id}^k + v_{id}^{k+1} \tag{13}$$

Where D represents the dimensionality of the particle; N denotes the number of particles in the swarm; X_i and V_i represent the position and velocity of the i-th particle, respectively; w is the inertia factor; c_1 and c_2 are the learning factors; r_1 and r_2 are random numbers distributed between 0 and 1; k is the iteration count; $pbest_i^k$ is the individual optimal solution for the i-th particle at the k-th iteration; and $gbest^k$ is the global optimal solution at the k-th iteration.

Compared to other optimization algorithms, this algorithm is suitable for high-dimensional optimization problems and demonstrates good convergence for seeking resilience enhancement strategies in complex networks. In addition, the algorithm has strong global search capabilities, it prevents the results from being trapped in local optima. Moreover, the approach can be adjusted based on variations in engineering requirements and resource conditions. It can be combined with other techniques, making it applicable to optimization problems in engineering systems.

To ensure that the results obtained after multiple iterations are the global optimal solution, we establish a global optimum criterion. We consider the optimization process complete if the global optimal solution remains unchanged after 100 consecutive iterations, and the final results are the global optimal solutions.

A pre-typhoon resilience improvement framework based on economic constraints is presented, as shown in Fig. 4. First, wind-resistant enhancement plans and initial parameters of the algorithm are set. Initial strategies are randomly selected based on the economic budget. Subsequently, each strategy is simulated to obtain the resistance-based resilience metrics. In this method, the failure probability of infrastructure under the implementation of strategy can be clarified. The Monte Carlo method is employed to simulate the network function model and assess the system's functional metrics. After reaching the required number of random samples, the expected values of the system's functional metrics are output. The typhoon's duration and monitoring time intervals to obtain the functional time-varying curve $K_{res}(t)$, thus enabling the evaluation of the resistance-based resilience metrics. Then, the optimal strategy is selected and updated to generate new strategies that meet economic constraints. Multiple iterations of simulation are performed until the global optimum criterion is met. The globally optimal parameters are output, representing the wind-resistant enhancement strategies.

3.2. Post-typhoon resilience improvement

Numerous infrastructures and complex power transmission paths make the system recovery process highly intricate. Therefore, it is crucial to identify the key components of power systems under typhoons and prioritize the repair of infrastructure. The recovery path strategy helps maximize the recovery of power systems within the constraints of limited resources and time.

The emergency repair resources for power systems include repair teams, machinery, and transport vehicles. These resource conditions directly affect the recovery efficiency. However, in practical engineering, there is uncertainty regarding whether repair resources can meet the demands of post-disaster restoration. Therefore, it is important to rationally allocate restoration resources to maximize economic benefits in the absence of sufficient repair teams and machinery.

The recovery strategy determines the functional time-varying curve of power systems after a typhoon. Owing to the limitations of repair resources, it is necessary to optimize the recovery strategy to improve repair efficiency. Therefore, we propose the recovery-based resilience metrics R_{rec} to measure the system's recovery capability under different post-typhoon recovery path strategies, as shown in Eq. (14). Moreover, given the constraints on repair resources, we need to optimize the allocation of these resources to improve the system recovery efficiency. We introduced the resource investment efficiency S_e, as shown in Eq. (15). Where $K_{rec,\ a}(t)$ and $K_{rec,\ b}(t)$ represent the functional time-varying curves after and before applying the resource allocation strategy; S_a and

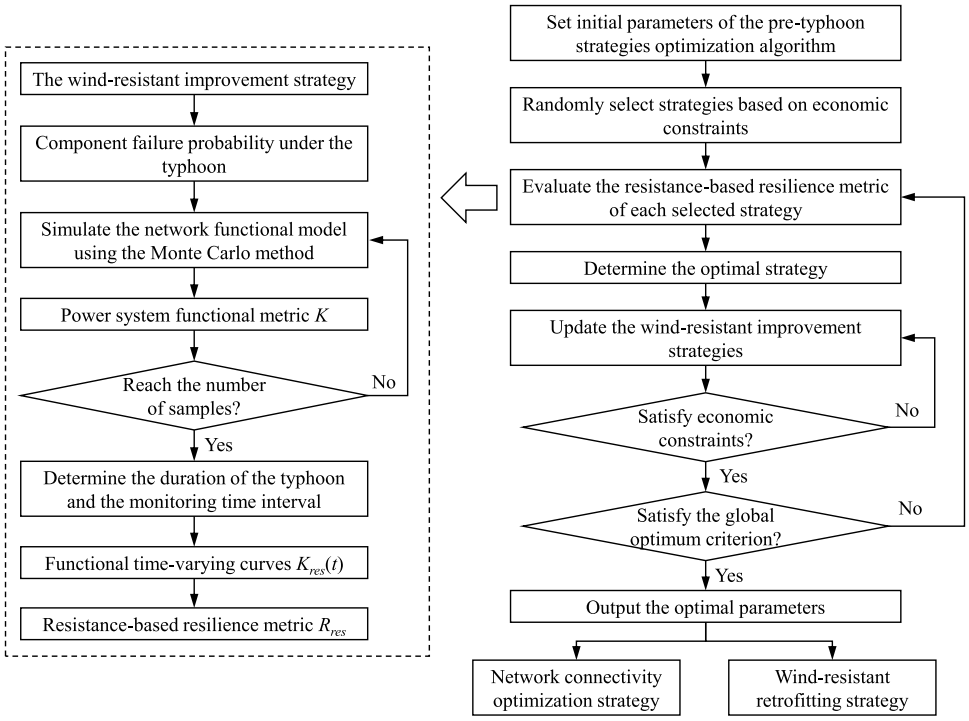

Fig. 4. Pre-typhoon resilience improvement framework based on economic constraints.

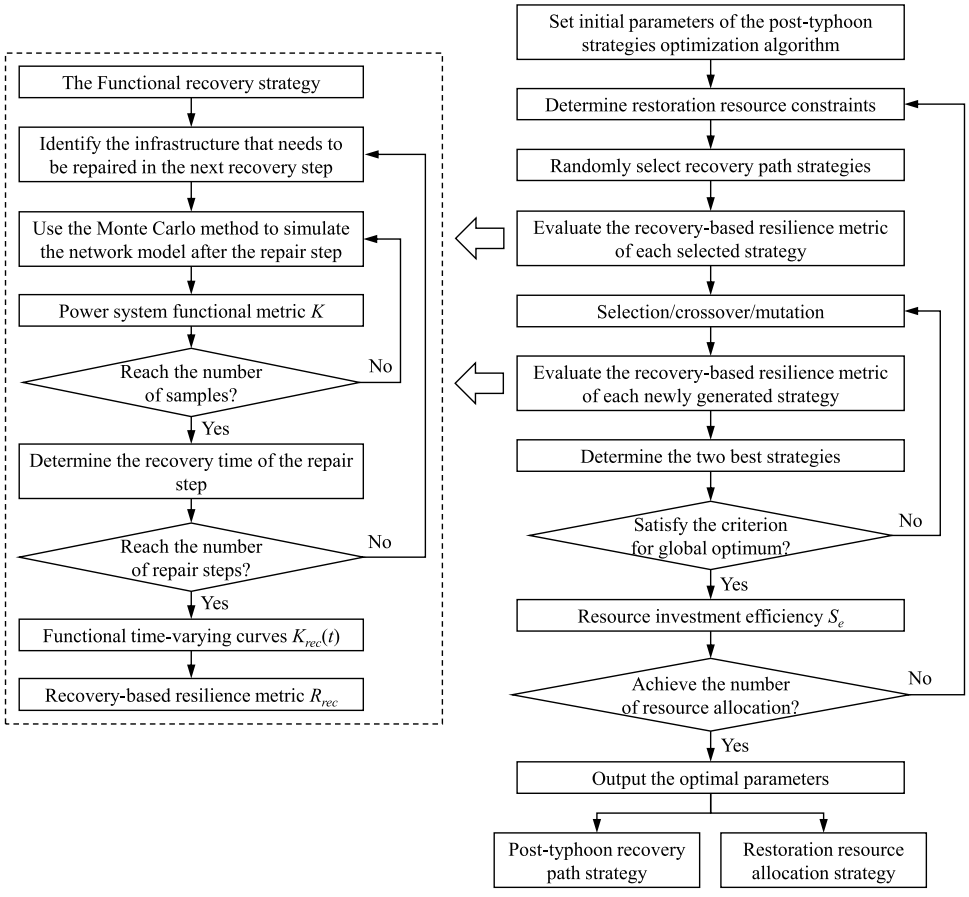

Fig. 5. Post-typhoon resilience improvement framework based on resource constraints.

S_b represent the resource inputs after and before the allocation strategy, respectively.

$$R_{rec} = \int_{T_r}^{T_c} (100 - K_{rec}(t))dt \tag{14}$$

$$S_e = \frac{\int_{T_r}^{T_c} (K_{rec,a}(t) - K_{rec,b}(t))dt}{S_a - S_b} \tag{15}$$

The recovery path after a typhoon is continuous and cannot be simplified into particles for position and velocity updates. Therefore, the previously mentioned optimization algorithm is unsuitable. To optimize the post-typhoon recovery path strategy, a genotype-based strategy optimization algorithm is proposed. In this approach, the recovery path is represented as a genotype, each repair sequence corresponds to a genetic sequence. The recovery-based resilience metrics are defined as the fitness value to evaluate the quality of the genetic sequence. The algorithm gradually optimizes the solution over generations through selection, crossover, and mutation of genetic sequences, ultimately identifying the optimal post-typhoon recovery path strategy. This algorithm improves the global search range through crossover and mutation, it also has good applicability for parameter optimization problems with multiple constraints. Additionally, the optimization results of this approach are independent of the initial parameters. This algorithm can achieve improved convergence efficiency by increasing the size of the initial population.

A post-typhoon resilience improvement framework based on resource constraints is proposed, as shown in Fig. 5. First, the operational states of the power infrastructure are clarified after the typhoon, and the initial parameters of the optimization algorithm are set. Restoration-resource allocation constraints are established, followed by the random selection of recovery paths to evaluate the recovery-based resilience metrics. Specifically, each recovery step within the recovery path is identified for the power infrastructure. Monte Carlo simulations are used to assess the functional metrics of the repaired power system, as well as the repair time for the recovery step. Then, the network functional model is updated. The next repair step is simulated until all repairs are completed. This results in the functional time-varying curve $K_{rec}(t)$, allowing for the evaluation of the recovery-based resilience metric. Simulations are conducted for all recovery strategies using this method. Employing selection, crossover, and mutation to identify two sets of optimal solutions. Iterative propagation continues until the global optimum criterion is satisfied. The recovery path and resource investment efficiency under the given repair resource constraints are determined. Finally, altering the resource-allocation constraints and re-simulating to obtain the optimal recovery strategy.

4. Case study

4.1. IEEE RTS-79 test system

The Institute of Electrical and Electronics Engineers introduced the Reliability Test System in 1979 (IEEE RTS-79). To evaluate the applicability of the framework proposed in this study, we selected this IEEE RTS-79 for assessing the resilience improvement. Although this model is not an actual engineering network, it can be used to test or compare methods for resilience analysis and simulation of power systems [44]. The network diagram of the IEEE RTS-79 is shown in Fig. 6. It contains 24 units connected by 38 lines at two voltages (230 kV and 138 kV). The units in the power system include ten groups of power plant units, six groups of substation units, and eight groups of bus units. Most units are load units. The total transmission load level is 2850 MW. The lines in the IEEE RTS-79 are composed of transmission tower-line systems, with a tower height of 44 meters and a distance of 400 meters between adjacent towers. The length (km) of the lines between each group of units is marked in red.

To evaluate the operational states of infrastructures in the IEEE RTS-79, we reference literature [45] to obtain the fragility curves for various types of infrastructure. The reports regarding power plants are limited. Because both power plants and substations are classified as engineering network systems with strong wind resistance capabilities, we assume

Table 1
Fragility curve parameters for power plants and substations (IM: Wind speed).

Functional state k	μ	β
Moderate(40 %)	5.068	0.136
Severe(70 %)	5.204	0.147
Complete(100 %)	5.523	0.132

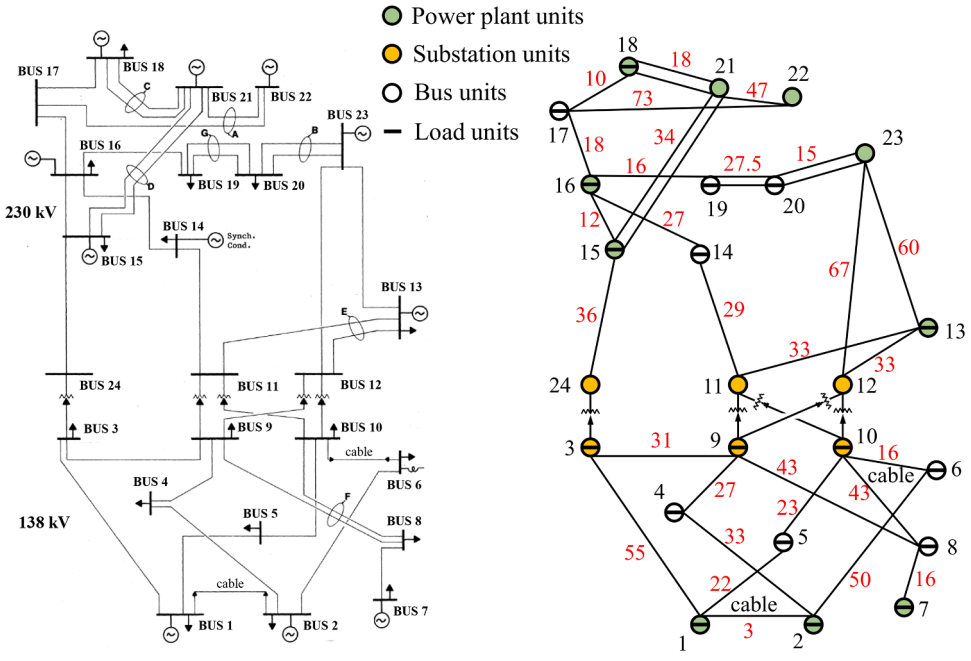

Fig. 6. Network diagram of the IEEE RTS-79.

that both share the same fragility curve parameters. The infrastructure's functionality is classified according to the damage states and quantities of equipment, with specific parameters listed in Table 1. The numbers in parentheses represent the functional states of the infrastructure. The transmission tower-line system is significantly affected by wind direction and wind speed. The member of diagonal or secondary braces reaching the plastic state is considered as the criterion for structural damage [46], the fragility curve parameters of the transmission towers are obtained, as shown in Table 2. In addition, the recovery processes of various infrastructures are uncertain. The experience of repair personnel and relevant literature shows that the repair time of equipment generally follows a normal distribution [47,48]. Therefore, the repair time parameters for different types of infrastructure are obtained [20,49], as shown in Table 3, where θ represents the median and σ represents the standard deviation.

4.2. A typical typhoon case

This study uses the power system and typhoon conditions around Quanzhou, China, as a case study. Based on data provided by the Typhoon Center of the China Central Meteorological Observatory, we extracted the movement trajectory and parameters of Typhoon "DOKSURI" when it made landfall in Quanzhou in 2023, as shown in Fig. 7 and Table 4. The meteorological monitoring interval for Typhoon "DOKSURI" was set at 3 hours.

4.3. System functional state during the typhoon

In the latest research techniques for disaster simulations of power systems, the simulation results vary depending on the adopted methodology. Yang et al. adopted a data-driven approach to build a transmission corridor model and evaluated the fault correction rate of the transmission corridor. However, the data-driven approach requires the collection of a large amount of regional disaster sample data [31]. Wang et al. established a probability model for the outage of transmission branches under typhoons. They proposed a preventive islanding scheme using genetic algorithms. This research focused on the preventive islanding effect of power systems during typhoons, particularly on the feasibility of evaluating the operation of the post-disaster power systems. However, this technology did not pay attention to the dynamic recovery process of the functional state of power systems after typhoons [40]. Moreover, some research techniques require extensive runtime and data processing [50]. Therefore, this study employs undirected weighted graphs and adjacency matrices to quickly assess the working states of the power system. To reduce the disaster simulation time, the operational state of the IEEE RTS-79 was simulated using the Monte Carlo method. We took the average value of 20,000 Monte Carlo sampling results as the reference value. Because the computational workload for 20,000 samples is substantial, we reduce the number of samples. If the deviation between the average value of the samples and the reference value is less than 2 %, the results were considered to converge well. We found that 1,000 Monte Carlo samples meet this convergence criterion, so the number of samples for subsequent simulations is set to 1,000.

The time-varying curve of functional loss for the IEEE RTS-79, $K_{res}(t)$,

Table 2
Fragility curve parameters for transmission tower-line systems (IM: Wind speed).

Direction(°)	μ	β
0	3.153	0.053
22.5	3.261	0.051
45	3.612	0.052
67.5	3.665	0.053
90	3.730	0.062

Table 3
Repair time parameters for different types of infrastructure (unit: day).

Parameter	Power plant units	Substation units	Tower-line system
θ	65	30	3
σ	30	15	1

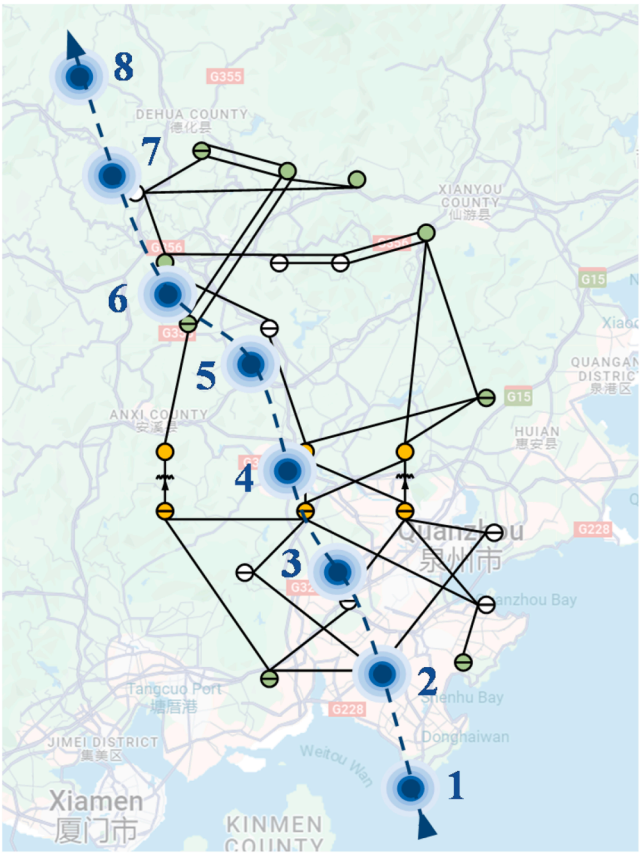

Fig. 7. Movement trajectory of typhoon "DOKSURI".

Table 4
Movement parameters of typhoon "DOKSURI".

Location	1	2	3	4	5	6	7	8
ΔH(hPa)	78	73	63	53	43	33	28	25
ψ (°)	24.3	24.7	24.9	25	25.4	25.5	25.8	26
V_m (km/h)	24	25	30	30	30	33	30	30

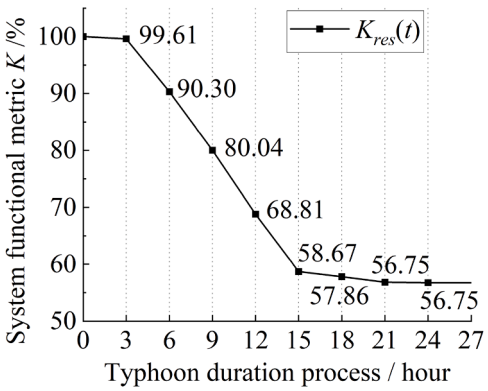

Fig. 8. Time-varying curve of functional loss for the IEEE RTS-79.

is shown in Fig. 8. It shows that the power system experiences significant functional loss within the first 15 hours of the typhoon's impact. This indicates the destructive effect of typhoons on the power system. As the typhoon's intensity decreases, the functional loss of IEEE RTS-79 stabilizes, and the system's functionality eventually settles at 56.75 %. The simulation provides a quantitative assessment of the system's time-varying functional loss.

The operational states of infrastructure within the IEEE RTS-79 under the typhoon are shown in Fig. 9. The red markings indicate the transmission line numbers. Because power plants and substations have stronger wind resistance compared to transmission towers, they did not experience obvious damage during Typhoon "DOKSURI." Additionally, the damage degree to transmission lines varies. We assume that if fewer than three sets of transmission towers are damaged along a transmission line, it is considered a slightly damaged line, and other cases are classified as severely damaged lines. Fig. 9 shows that transmission lines located along the typhoon's movement trajectory are severely damaged. In particular, the operational states of long-distance power transmission lines are more vulnerable to the impact of the typhoon.

5. Optimization and discussions

The resilience improvement was optimized from four dimensions: spare-line configuration, wind-resistant reinforcement for transmission lines, post-typhoon recovery path, and restoration-resource allocation strategies. The optimal strategies under specific economic and resource constraints were identified. Although the pre-typhoon strategies proposed in this study are optimized measures derived from simulation analyses based on past disasters, these solutions and strategies still play a significant role in addressing future uncertain events. Current technologies are unable to accurately predict the intensity and movement trajectory of typhoons several weeks or even months in advance, making it impossible to implement pre-typhoon strategies for future typhoon occurrences. At present, most pre-typhoon response measures for power grid systems take into account factors such as the cost of infrastructure and equipment, engineering experience, and historical disaster data. Therefore, this study aims to summarize the optimal combinations of pre-disaster measures under previous typhoon disasters and identify the general measures of such strategies, thereby providing references for disaster prevention and mitigation under future uncertain events.

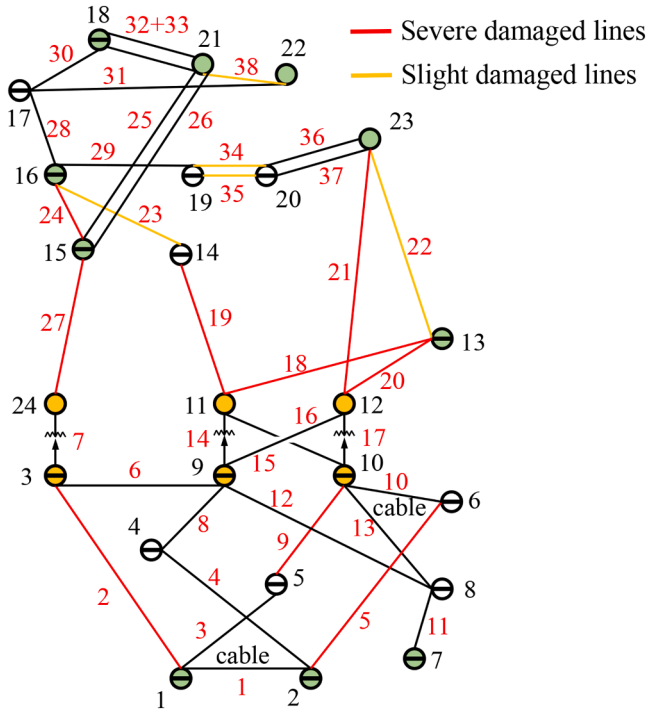

Fig. 9. Operational states of infrastructure in the IEEE RTS-79.

5.1. Spare-line configuration optimization

A total of 14 transmission lines are damaged in the IEEE RTS-79, of which 5 lines (Lines 22, 23, 34, 35, 38) suffer slight damage. Given sufficient repair personnel, the recovery time for these slightly damaged lines is relatively short, and their impact on the power system is minimal. Therefore, we focus on the spare-line configuration plans for the nine severely damaged transmission lines. Because the terrain and geology between various types of infrastructure may not guarantee successful power transmission, we do not alter the network connectivity structure of the IEEE RTS-79. Instead, we focus on adding and configuring spare lines to the existing transmission lines.

A strategy optimization algorithm based on the particle swarm was used to find the spare-line configuration plan for the IEEE RTS-79. The initial parameters of the optimization algorithm are set as shown in Table 5. The particle dimension is determined by these 9 severely damaged transmission lines (Lines 2, 5, 9, 18, 19, 20, 21, 24, 27). The search range for each iteration is expanded by increasing the swarm size. The other initial parameters are set values and do not affect the global optimal solution.

The spare transmission lines are only used in emergencies, so we assume that the spare lines will not be damaged simultaneously with the regular lines. Referring to the cost information from the China National Energy Administration's Power Engineering Cost Information website, the cost of transmission lines in 2022 is estimated to be approximately $190,000 per kilometer. To ensure the wind resistance of the spare lines, we assume that the cost of the spare lines is the same as that of the regular lines. Given the high economic cost of adding spare lines, we assume five economic budget scenarios ($E_{B\text{-}S}$): $5 million (M), $10 M, $15 M, $20 M, and $25 M. Through optimization simulation of the IEEE RTS-79, the spare-line configuration strategies are shown in Table 6, and the time-varying functional state is shown in Fig. 10.

Table 6 shows that as the economic budget increases, the spare-line configuration strategy is not completely redesigned but rather builds upon the existing strategy by adding new spare lines. This indicates that the variation in economic budget does not change the importance of the spare lines. Fig. 10 shows that increasing the economic budget for spare lines enhances the power system's wind resistance during typhoons. When $25 M is invested in adding spare lines, the resilience metric (R_{res}) of the IEEE RTS-79 decreases by approximately 41 %, significantly improving the system's functional resilience.

5.2. Wind-resistant retrofitting optimization

Fragility curves were used to represent the wind-resistant reliability of electrical infrastructure. Therefore, we use the increase in the median value of the infrastructure's fragility curve to reflect the degree of wind-resistant reinforcement. This method can be adjusted based on the differences in reinforcement methods and degrees, making it highly adaptable. Because the damaged infrastructure in the IEEE RTS-79 primarily consists of transmission towers, references [51,52] show that reinforcement methods for transmission towers mainly involve adding stiffening ribs and diagonal braces to the main legs and diagonal members. Based on the repair costs for transmission towers, three wind-resistant reinforcement plans and their costs are proposed in Table 7. Although the plans in Table 7 differ from actual engineering

Table 5
Initial parameters of the optimization algorithm based on the particle swarm.

Parameter	Particle dimension	Swarm size	c_1	c_2	w
Value	9	10	1.5	1.5	0.6

Table 6
Spare-line configuration strategies for the IEEE RTS-79.

$E_{B\text{-}S}$ (million)	Specific measures
5	L9
10	L9/L19
15	L9/L19/L24
20	L9/L19/L20/L24
25	L9/L18/L19/L20/L24

* L represents transmission lines.

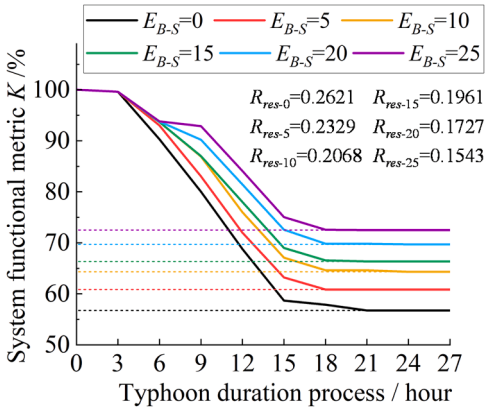

Fig. 10. Functional time-varying curves under spare-line configuration strategies.

Table 7
Wind-resistant reinforcement plans and costs for transmission towers.

Serial number	Cost (thousand)	Median increase
1	25	20 %
2	50	30 %
3	75	35 %

practices, they are essential for conducting wind-resistant reinforcement optimization in this research. Once specific wind-resistant reinforcement methods and parameters in practical engineering are clarified, they can be easily integrated into the optimization framework proposed in this study for case analysis, leading to more accurate wind-resistant reinforcement optimization solutions.

The economic costs of reinforcing transmission lines are significantly lower than the costs of adding spare transmission lines. Therefore, we assume five economic budget scenarios for reinforcement ($E_{B\text{-}R}$): \$3 M, \$6 M, \$9 M, \$12 M, and \$15 M. Through optimization simulations of the IEEE RTS-79, the wind-resistant retrofitting strategies for the transmission lines are presented in Table 8, where the serial number of reinforcement plans used for each transmission line is indicated in parentheses. The functional time-varying state of the IEEE RTS-79 is illustrated in Fig. 11.

Table 8 shows that the number of reinforced transmission lines increases as the economic budget grows. This indicates that reinforcing more transmission lines is more effective than continuously reinforcing a single transmission line. Fig. 11 illustrates that the retrofitting

Table 8
Wind-resistant retrofitting strategies for the IEEE RTS-79.

$E_{B\text{-}R}$ (million)	Specific measures
3	L9(1)/ L18(1)/L19(1)/L20(1)
6	L5(1)/L9(2)/ L18(1)/L19(1)/L20(1)/ L24(1)/ L27(1)
9	L2(1)/L5(1)/L9(1)/L18(1)/L19(1)/L20(1)/ L21(1)/L24(2)/L27(1)
12	L2(1)/L5(1)/L9(2)/L18(2)/L19(2)/L20(2)/ L21(1)/L24(3)/L27(1)
15	L2(2)/L5(1)/L9(3)/L18(2)/L19(2)/L20(2)/ L21(1)/L24(3)/L27(2)

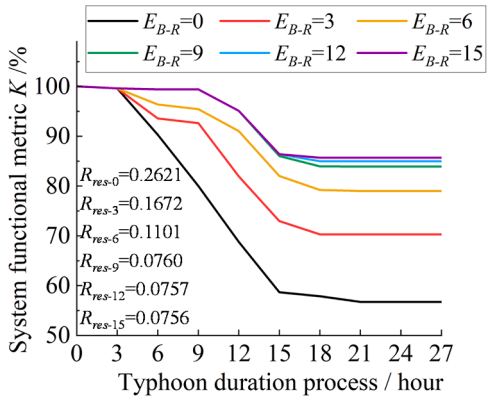

Fig. 11. Functional time-varying curves under wind-resistant retrofitting strategies.

efficiency decreases as the economic investment increases. When the economic investment for wind-resistant reinforcement is \$9 M, the resilience metric (R_{res}) decreases by approximately 71 %, this is significantly better than the effect of adding spare lines. Furthermore, when the economic investment for wind-resistant reinforcement exceeds \$9 M, the retrofitting effectiveness of these nine transmission lines becomes less pronounced. This shows that random damage to other infrastructure also impacts the operational state of the IEEE RTS-79.

To compare our research results with the latest techniques, Tari et al. used the amount of energy not supplied and the value of lost load as key metrics to evaluate the effectiveness of hardening strategies. They also assessed the associated costs [27]. Although their proposed hardening algorithm is effective, the measures are standardized and uniform, resulting in slower convergence when applied to complex scenarios and diverse reinforcement forms. Hou et al. employed the resilience achievement worth to assess the importance of infrastructure [28]. However, the reinforcement measures for infrastructure were manually predetermined. The optimal hardening strategies were identified, but the differences among various types of infrastructure reinforcement were not fully captured. To clarify the effectiveness of the wind-resistant retrofitting strategy proposed in this study, we randomly generated 100 sets of reinforcement measures under different economic budgets ($E_{B\text{-}R}$). The average resilience metrics $R_{res(a)}$ and the optimal resilience metrics $R_{res(b)}$ resulting from the 100 sets of random reinforcement measures are shown in Table 9.

Table 9 shows that the resilience metrics of the optimal wind-resistant retrofitting strategies are significantly lower than that of the random retrofitting strategies, thereby demonstrating both the effectiveness of the optimization algorithm and the importance of the proposed optimization strategies. Here, the optimization simulation was conducted using a 13th Generation Intel Core i9-13900HX processor and an RTX 4060 graphics card. Each set of strategy optimization simulations took less than 15 seconds, highlighting the high efficiency of the data optimization in this study.

5.3. Post-typhoon recovery path optimization

To quantitatively assess the recovery process of the IEEE RTS-79, we assume that a repair team consists of 20 repair personnel and lifting equipment. A single repair team cannot simultaneously restore multiple groups of infrastructure, and the repair of the next infrastructure can

Table 9
Resilience metrics after 100 sets of random reinforcement measures.

$E_{B\text{-}R}$	300	600	900	1200	1500
$R_{res(a)}$	0.2236	0.1710	0.1590	0.1311	0.1089
$R_{res(b)}$	0.1672	0.1101	0.0760	0.0757	0.0756

only begin after the complete restoration of the previous infrastructure. Because we focus primarily on recovery path optimization rather than resource allocation in this section, we assume that only one repair team is engaged in the restoration work, working 12 hours a day, with the remaining time allocated for equipment transportation and personnel rest.

The repair time for slightly damaged transmission lines is relatively short. Therefore, we should prioritize the repair of slightly damaged transmission lines to quickly restore partial connectivity of the power system. For the severely damaged transmission lines, it is necessary to determine the post-typhoon recovery path to improve repair efficiency. The genotype-based strategy optimization algorithm was used to find the recovery path strategy for the IEEE RTS-79. The initial parameters of the optimization algorithm are shown in Table 10. The recovery path strategies and the functional time-varying state of the IEEE RTS-79 were obtained through optimization simulations, as shown in Fig. 12(a). The labels indicate the repair sequence of transmission lines in the functional time-varying curve; SDL represents the slightly damaged lines. Although the research techniques of Ouyang et al. involved post-disaster restoration models [20], they did not clearly specify the priority of restoration for specific substations and transmission lines. This is a common issue in previous studies [53]. To further refine the latest research techniques and results, we assumed random restoration of damaged transmission lines and obtained the resilience metrics R_{rec} as shown in Fig. 12(b).

Fig. 12(a) shows that the initial repair efficiency of the power system is high. Additionally, prioritizing the repair of short-distance transmission lines connected to substations is more effective. Because the resistance-based resilience metrics are much lower than the recovery-based resilience metrics, the power system's post-typhoon recovery capability plays a crucial role in influencing the resilience metrics. Moreover, Fig. 12(b) shows that the resilience metrics for random recovery paths are much higher than that for the optimal recovery path. The median resilience metric R_m and the average resilience metric R_a are 15.14 and 15.54, respectively. The lowest resilience metric (R_l) and highest resilience metric (R_h) obtained from random sampling show significant differences. This indicates that explicitly specifying the repair priorities for individual substations and transmission lines is necessary, demonstrating the effectiveness of our proposed methodology.

5.4. Restoration-resource allocation optimization

The number of repair personnel and lifting equipment directly impacts the recovery time of the power system. However, recent studies mainly focused on model construction and strategy optimization algorithms. Research on resource allocation has mostly adopted simplified quantification. Some scholars have even assumed that resource allocation fully meets engineering demands. To conduct an optimization analysis of resource allocation, we assume five restoration resource scenarios: 2, 3, 4, 5, and 6 repair teams (N_{RT}), with no collaboration between the teams. We simulated the allocation of repair resources based on this recovery path. The functional time-varying state and the resource investment efficiency (S_e) are shown in Fig. 13.

Fig. 13 shows that multiple repair teams can significantly shorten the post-typhoon recovery time, thereby reducing the resilience metrics. However, the increase in repair teams leads to a gradual decline in resource investment efficiency. Therefore, in practical engineering, the optimal configuration of repair teams should be determined based on the extent of damage to the power system and the specific recovery goals.

Table 10
Initial parameters of the genotype-based strategy optimization algorithm.

Parameter	Population size	Crossover probability	Mutation probability
Value	10	0.8	0.05

5.5. Multi-strategy correlation and optimization

To maximize the wind resistance and post-typhoon recovery capabilities of the IEEE RTS-79, we combine the four dimensions of resilience improvement strategies. Because the pre-typhoon preventive strategies and the post-typhoon recovery strategies are continuous. The purpose of the multi-strategy research is to explore the promoting or restrictive relationships among different pre-typhoon preventive strategies and follow up on their impacts on post-typhoon recovery strategies. Therefore, multi-dimensional strategies cannot be treated as an all-in-one problem. In this case, we assume that four repair teams are available for post-typhoon recovery, with an economic budget of $10 M. The optimal combination of multi-dimensional strategies was obtained through resilience assessment, as shown in Table 11.

Table 11 shows that the entire economic budget is allocated to wind-resistant reinforcement of transmission lines rather than adding spare lines. Because the cost of wind-resistance reinforcement is significantly lower than that of adding spare lines, and the reinforced transmission lines will not be damaged under this typhoon. Therefore, reinforcing multiple transmission lines offers the highest economic benefit. The recovery path strategy and the reinforced transmission lines are completely different, further proving that the reinforced lines will not be damaged. However, this does not imply that adding spare lines is unnecessary. In other typhoon scenarios, reinforced transmission lines may suffer damage. In addition, for transmission lines serving critical power users, adding spare transmission lines is essential. Therefore, the specific settings of this strategy need to be determined based on the typhoon scenario and practical engineering.

To quantitatively assess the resilience improvement effects of the optimal combination of multi-dimensional strategies for the IEEE RTS-79, we compared the system functional time-varying curves before and after implementing the strategies, as shown in Fig. 14. We assumed that the decision-making and deployment time after the typhoon is 3 hours. Because the duration of the typhoon is much shorter than the recovery time of the power system, a logarithmic function is used to represent the X-axis coordinates, thereby reflecting the function loss and the recovery process.

Fig. 14 shows that the optimal combination of multi-dimensional strategies significantly improves the post-typhoon residual functionality (K_R) of IEEE RTS-79. The strategies reduce the recovery time (T_c) to less than three days. As a result, the resilience metric decreases by 95.6 %. In addition, we assume that the economic loss from a power outage for power users is $4.76 per kWh [12,20,54]. The economic loss from a one-day power outage in the power system is approximately $325 million after calculations. By adopting the optimal combination of multi-dimensional strategies, the economic loss can be reduced by $1.59 billion, which is far less than the $10 M budget for economic investment. This demonstrates the optimization efficiency and effectiveness of the proposed strategies. In practical engineering networks, the optimal combination of strategies should be formulated based on the wind-resistance capabilities of the power system and regional economic conditions.

6. Conclusions

In this study, the operational states and resilience of power systems under typhoon conditions were conducted. The resilience improvement strategies were analyzed using a typical power-network test system. The main conclusions are as follows.

1) A resilience assessment method for power systems under typhoons was developed. First, a typhoon wind-field model was constructed, and fragility curves were used to evaluate the operational states of infrastructures. Power systems were represented as undirected weighted graphs, with infrastructure operational states and network connectivity stored in an adjacency matrix. This method facilitates

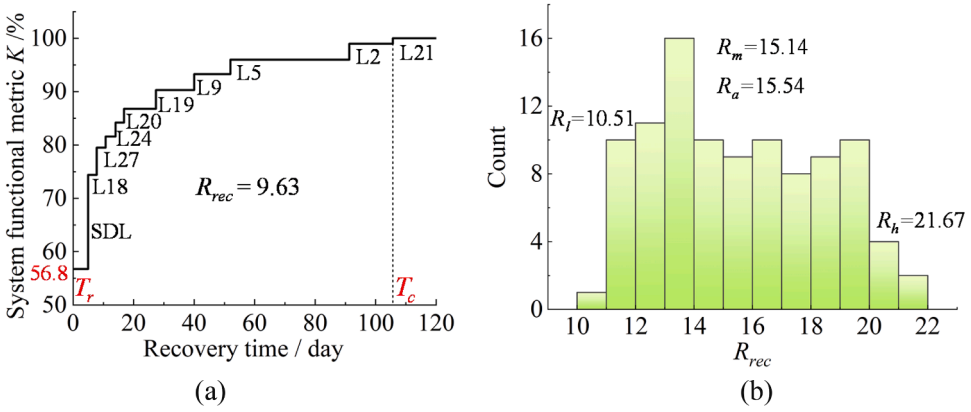

Fig. 12. (a) Recovery path strategies and the functional time-varying state, (b) Distribution of resilience metrics for randomly selected recovery paths.

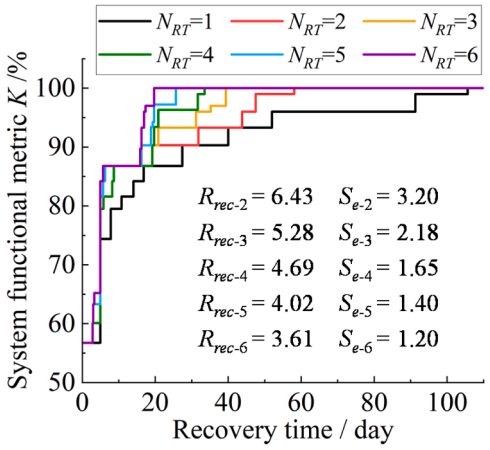

Fig. 13. Functional time-varying state and the resource investment efficiency.

Table 11
Optimal combination of multi-dimensional strategies for the IEEE RTS-79.

Resilience improvement strategies	Specific measures
Spare-line configuration	No additional spare transmission lines
Wind-resistant reinforcement	L2(1)/L5(1)/L9(1)/L18(2)/L19(1)/L20(1)/ L21(1)/ L24(3)/L27(1)
Post-typhoon recovery path	L12-L10-L13-L23-L22-L34-L38

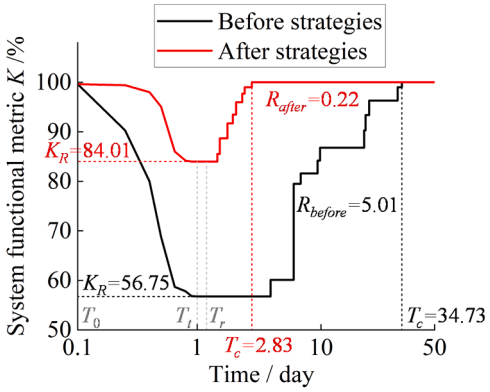

Fig. 14. Functional time-varying curves before and after implementing the strategies.

the updates of the system's states through matrix operations during simulations. System functional metrics were established based on three dimensions: power transmission efficiency, reliability, and load capacity. Time-varying curves were analyzed, and the resilience was quantitatively assessed.

2) A resilience improvement framework based on strategies optimization of power systems was proposed. Four-dimensional strategies were developed for both pre- and post-typhoon stages. Considering economic constraints, a strategy optimization algorithm based on the particle swarm was introduced. The identification of network fragilities was achieved to improve the system's wind resistance. Subsequently, a post-typhoon recovery strategy optimization algorithm was designed. The critical components for repair under different resource allocation scenarios were identified to improve the system's recovery efficiency.
3) A resilience assessment of a typical power-network test system was conducted from four dimensions: spare-line configuration, wind-resistant reinforcement, repair path, and restoration-resource allocation strategies. Optimal solutions for each resilience improvement strategy were identified, and the critical infrastructures for reinforcement and recovery were determined. Given the interrelation of these strategies, we explored the optimal combination of multi-dimensional strategies under specific economic budgets and resource constraints, thereby maximizing the resilience improvement and ensuring the safety of power systems.

The resilience improvement framework proposed in this study can improve the cost-effectiveness of pre-disaster measures and post-disaster resource utilization for practical engineering. Additionally, the structural characteristics of engineering networks such as transportation and water supply share similarities with this study. Therefore, the resilience improvement framework can be extended and applied to various systems based on their operational features, thereby demonstrating its engineering value.

However, the infrastructure fragility parameters and repair time parameters were obtained from the previous literature, and the resilience assessment method established has certain limitations. This may not be accurate in practical engineering. Additionally, to quantitatively assess the differences in resilience improvement strategies, certain assumptions were made regarding infrastructure costs and the work processes of repair teams. These may affect the evaluation results of the strategies. Therefore, adjustments should be made when applying them to real engineering scenarios. In future research, it is important to seek newer, more general, and more informative metrics for measuring resilience, as they play a crucial role in advancing the quantitative assessment of disaster resistance in engineering systems. In addition, the typhoon disaster early warning and monitoring platform should be integrated with the infrastructure resilience assessment framework to

achieve state assessment and strategy formulation under accurate prediction of future typhoon scenarios. Moreover, utilizing artificial intelligence for scheduling to address changes in supply and demand in engineering is an important research direction for advancing intelligent adaptive power systems.

CRediT authorship contribution statement

Xiao Liu: Writing – original draft, Software, Methodology, Funding acquisition, Formal analysis, Data curation. **John S. Owen:** Validation, Supervision, Software, Methodology, Formal analysis, Conceptualization. **Qiang Xie:** Supervision, Resources, Project administration, Investigation, Funding acquisition, Data curation, Conceptualization. **Tiantian Wang:** Validation, Resources, Investigation, Funding acquisition, Data curation.

Declaration of competing interest

The authors declare that they have no known competing financial interests or personal relationships that could have appeared to influence the work reported in this paper.

The authors declare that they have no financial interests/personal relationships which may be considered as potential competing interests.

Acknowledgements

This study was financially supported by the National Natural Science Foundation of China (Grant No. 51878508) and China Scholarship Council (Grant Nos. 202306260184 and 202306260201). The grants are greatly appreciated.

Data availability

Data will be made available on request.

References

[1] Dai KS, Chen SE, Luo MY, Loflin Jr G. A framework for holistic designs of power line systems based on lessons learned from Super Typhoon Haiyan. Sustain Cities Soc 2017;35:350–64.
[2] Chung SY, Xu Y. Reliability and resilience in a regulated electricity market: Hong Kong under Typhoon Mangkhut. Util Policy 2020;67:101134.
[3] Liu W, Song ZY, Ouyang M, Li J. Lifecycle operational resilience assessment of urban water distribution networks. Reliab Eng Syst Saf 2020;198:106859.
[4] Bešinović N, Nassar RF, Szymula C. Resilience assessment of railway networks: combining infrastructure restoration and transport management. Reliab Eng Syst Saf 2022;224:108538.
[5] Xiao YH, Zhao XD, Wu YP, et al. Seismic resilience assessment of urban interdependent lifeline networks. Reliab Eng Syst Saf 2022;218:108164.
[6] Hosseini S, Barker K, Ramirez-Marquez J. A review of definitions and measures of system resilience. Reliab Eng Syst Saf 2016;145:47–61.
[7] Cimellaro GP, Renschler C, Reinhorn A, et al. PEOPLES: a framework for evaluating resilience. J Struct Eng 2016;142(10):04016063.
[8] Kammouh O, Gardoni P, Cimellaro G P. Probabilistic framework to evaluate the resilience of engineering systems using bayesian and dynamic bayesian networks. Reliab Eng Syst Saf 2020;198:106813.
[9] Omogoye O.S, Folly K.A, Awodele K.O. Review of sequential steps to realize power system resilience. In 28th South African Universities Power Engineering Conference, Mechatronics/Pattern Recognition Association (SAUPEC/RobMech/PRASA), Cape Town, South Africa, January 29-31, 2020.
[10] Liu JC, Tian L, Yang M, Meng XR. Probabilistic framework for seismic resilience assessment of transmission tower-line systems subjected to mainshock-aftershock sequences. Reliab Eng Syst Saf 2024;242:109755.
[11] Liu X, Xie Q, Liang H, Zhu W. Seismic resilience evaluation and retrofitting strategy for substation system. Int J Electr Power Energy Syst 2023;153:109359.
[12] Liu X, Xie Q. A multi-model probabilistic framework to evaluate seismic resilience of UHV converter stations. Eng Struct 2024;300:117153.
[13] Zhu W, Xie Q. Machine learning chain models for multi-response prediction of electrical equipment in substation subjected to earthquakes. Eng Struct 2024;319:118815.
[14] Wen JY, Wang LQ, Li XX, Zhang YT, Wei Y. Non-contact automated identification of earthquake-induced micro damage in substation equipment system based on local damping parameter screening with a surrogate model. Reliab Eng Syst Saf 2026;266:111704.
[15] Nguyen CH, Owen JS, Franke J, et al. Typhoon track simulations in the North West Pacific: informing a new wind map for Vietnam. J Wind Eng Ind Aerodyn 2021;208:104441.
[16] Ma LY, Christou V, Bocchini P. Framework for probabilistic simulation of power transmission network performance under hurricanes. Reliab Eng Syst Saf 2022;217:108072.
[17] Wang F, Tian J, Shi CL, et al. A multi-stage quantitative resilience analysis and optimization framework considering dynamic decisions for urban infrastructure systems. Reliab Eng Syst Saf 2024;243:109851.
[18] Salman AM, Li Y, Stewart MG. Evaluating system reliability and targeted hardening strategies of power distribution systems subjected to hurricanes. Reliab Eng Syst Saf 2015;144:319–33.
[19] Zhang Y, Wu YF, Zhang F, et al. Application of power grid wind monitoring data in transmission line accident warning and handling affected by typhoon. Energy Rep 2022;8:315–23.
[20] Ouyang M, Dueñas-Osorio L. Multi-dimensional hurricane resilience assessment of electric power systems. Struct Saf 2014;48:15–24.
[21] Espinoza S, Panteli M, Mancarella P, Rudnick H. Multi-phase assessment and adaptation of power systems resilience to natural hazards. Electr Power Syst Res 2016;136:352–61.
[22] Liu X, Hou K, Jia H, Zhao J, Mili L, Mu Y, et al. A resilience assessment approach for power system from perspectives of system and component levels. Int J Electr Power Energy Syst 2020;118:105837.
[23] Oboudi MH, Mohammadi M. Two-stage seismic resilience enhancement of electrical distribution systems. Reliab Eng Syst Saf 2024;241:109635.
[24] Fang YP, Sansavini G. Optimum post-disruption restoration under uncertainty for enhancing critical infrastructure resilience. Reliab Eng Syst Saf 2019;185:1–11.
[25] Wu JX, Wang PF. Risk-averse optimization for resilience enhancement of complex engineering systems under uncertainties. Reliab Eng Syst Saf 2021;215:107836.
[26] Mahzarnia M, Moghaddam MP, Baboli PT, Siano P. A review of the measures to enhance power systems resilience. IEEE Syst J 2020;14(3):4059–70.
[27] Tari AN, Sepasian MS, Kenari MT. Resilience assessment and improvement of distribution networks against extreme weather events. Int J Electr Power Energy Syst 2021;125:106414.
[28] Hou GY, Muraleetharan K, Panchalogaranjan V, et al. Resilience assessment and enhancement evaluation of power distribution systems subjected to ice storms. Reliab Eng Syst Saf 2023;230:108964.
[29] Zhou Z, Wu Z, Jin T. Deep reinforcement learning framework for resilience enhancement of distribution systems under extreme weather events. Int J Electr Power Energy Syst 2021;128:106676.
[30] Yuan W, Wang JH, Qiu F, et al. Robust optimization-based resilient distribution network planning against natural disasters. IEEE Trans Smart Grid 2016;7(6):2817–26.
[31] Yang R, Li Y. Resilience assessment and improvement for electric power transmission systems against typhoon disasters: A data-model hybrid driven approach. Energy Rep 2022;8:10923–36.
[32] Shi QX, Liu WX, Zeng B, et al. Enhancing distribution system resilience against extreme weather events: concept review, algorithm summary, and future vision. Int J Electr Power Energy Syst 2022;138:107860.
[33] Liang YT, Lin SJ, Feng XY, et al. Optimal resilience enhancement dispatch of a power system with multiple offshore wind farms considering uncertain typhoon parameters. Int J Electr Power Energy Syst 2023;153:109337.
[34] Zhao TY, Tang YC, Li QM, Wang JP. Enhancing urban system resilience to earthquake disasters: impact of interdependence and resource allocation. Int J Crit Infrastruct Prot 2024;45:100673.
[35] Liu X, Xie Q. A probabilistic framework to evaluate seismic resilience of substations based on three-stage uncertainty. Reliab Eng Syst Saf 2024;249:110219.
[36] Liu X, Xie Q. Resilience-based post-earthquake recovery strategies for substation systems. Int J Disaster Risk Reduct 2023;96:104000.
[37] Wang SL, Guo ZY, Huang XD, Zhang JH. A three-stage model of quantifying and analyzing power network resilience based on network theory. Reliab Eng Syst Saf 2024;241:109681.
[38] Zhang WX, Shao CZ, Hu B, et al. Transmission defense hardening against typhoon disasters under decision-dependent uncertainty. IEEE Trans Power Syst 2023;38(3):2653–65.
[39] Matsui M, Ishihara T, Hibi K. Directional characteristics of probability distribution of extreme wind speeds by typhoon simulation. J Wind Eng Ind Aerodyn 2002;90(12-15):1541–53.
[40] Wang ZC, Wang ZP. A novel preventive islanding scheme of power system under extreme typhoon events. Int J Electr Power Energy Syst 2023;147:108857.
[41] Batts ME, Simiu E, Russell LR. Hurricane wind speeds in the United States. J Struct Div 1980;106(10):2001–16.
[42] Sharma N, Tabandeh A, Gardoni P. Resilience analysis: A mathematical formulation to model resilience of engineering systems. Sustain Resilient Infrastruct 2018;3(2):49–67.
[43] Sharma N, Tabandeh A, Gardoni P. Regional Resilience Analysis: A multi-scale approach to optimize the recovery of interdependent infrastructure. Comput-Aided Civ Infrastruct Eng 2020;35(12):1315–30.
[44] Subcommittee P M. IEEE reliability test system. IEEE Trans power appar syst 1979;(6):2047–54.
[45] Ranjbar H, Hosseini SH, Zareipour H. Hurricane induced damage scenario determination of transmission network components. IEEE Power Energy Soc Gen Meet (PESGM) IEEE 2020:1–5.
[46] Wang J, Li HN, Fu X, et al. Wind fragility assessment and sensitivity analysis for a transmission tower-line system. J Wind Eng Ind Aerodyn 2022;231:105233.

[47] Liu X, Xie Q. A multi-strategy framework to evaluate seismic resilience improvement of substations. Reliab Eng Syst Saf 2024;245:110045.
[48] Liu X, Xie Q, Liang H, Zhang X. Post-earthquake recover strategy for substations based on seismic resilience evaluation. Eng Struct 2023;279:115583.
[49] FEMA. HAZUS-MH 5.1 Hazus Earthquake model technical manual. Washington, D. C., USA: FEMA; 2022.
[50] Li YR, Ma LY, Zhai CH, et al. A probabilistic framework for assessing and enhancing the resilience of power systems to typhoon hazards. Reliab Eng Syst Saf 2026;265:111607.
[51] Xie Q, Zhang J. Experimental study on failure modes and retrofitting method of latticed transmission tower. Eng Struct 2021;226:111365.
[52] Liu CC, Yan Z, Jiang T, Guo T, Zou YB. Experimental study on failure modes of a transmission tower reinforced with clamps. Eng Fail Anal 2024;159:108151.
[53] Zhu W, Xie Q. Post-earthquake rapid assessment for loop system in substation using ground motion signals. Mech Syst Signal Process 2024;208:111058.
[54] LaCommare KH, Eto JH. Cost of power interruptions to electricity consumers in the United States (US). Energy 2006;31(12):1845–55.